

CBPF-NF-026/82

GEODESIC MOTION AND CONFINEMENT
IN GÖDEL'S UNIVERSE

by

M. Novello, I. Damião Soares and

J. Tiomno

Centro Brasileiro de Pesquisas Físicas/CNPq
Rua Xavier Sigaud, 150
22290 - Rio de Janeiro, RJ - BRASIL

GEODESIC MOTION AND CONFINEMENT IN GÖDEL'S UNIVERSE

M. Novello, I. Damião Soares and J. Tiomno

Centro Brasileiro de Pesquisas Físicas/CNPq
Rua Xavier Sigaud, 150
22290 Rio de Janeiro, RJ - BRASIL

ABSTRACT

We present a complete study of geodesic motion in Gödel's universe, using the method of the Effective Potential. It then emerges a clear physical picture of free motion and its stability in this universe. Geodesics of a large class have finite intervals in which the particle moves back in time ($\frac{dt}{ds} < 0$) without violation of causality. Gödel's geometry produces the important property of confinement for a large class of geodesics. We use this property to discuss the construction of a gravitational container. This structure is highly stable, since there is no singularity in its interior, and independent of the energy of the particles contained in it.

1. INTRODUCTION

In the present paper we analyse some remarkable properties of free motion of particles in a rotating universe. The most important feature of a rotating universe is that matter rotates with non-zero angular velocity, in the local inertial frames of its comoving observers. We limit our considerations here to Gödel's geometry [1] although our results could well be extended to other rotating Gödel-like models. Geodesic motion in Gödel's cosmos has been analysed independently by Kundt, and Chandrasekhar and Wright [2,3] more than twenty years ago, in which they found some weird properties of trajectories of the particles. In our search to understand completely the main features of Gödel's cosmos we decided to retake this problem in a complete new view. The basic difference between our treatment and the previous ones [2,3] rests in our use of the method of the *Effective Potential* by means of which we obtained not only their results but also gained a simpler characterization and a clear physical image of the structure of free motion of particles (massive and massless) in this space-time geometry.

We divide the paper as follows. In section II and III we present the equations of motion, the first integrals and we introduce the *Effective Potential*. The main properties of the *Effective Potential* - whose parametrization characterizes distinct families of geodesics - are presented. Section IV deals with the important property of confinement which Gödel's geometry produces, for a large class of geodesics. In section V, VI and VII we give the complete system of integrated expressions for geodesic curves and we draw some illustrative graphs of the

trajectories in the plane (r, ϕ) . Also the property of traveling back in time along a piece of some curves is examined. We conclude with Section VIII, where we discuss some fundamental properties of Gödel's geometry related to geodesic motion and possible applications.

II. THE EQUATIONS OF GEODESIC MOTION

In the cylindrical coordinate system (t, r, ϕ, z) the fundamental length of Gödel-like geometry is given by

$$ds^2 = a^2 \{ (dt + H(r)d\phi)^2 - dr^2 - dz^2 - R^2(r)d\phi^2 \} \quad (2.1)$$

For the case of Gödel's cosmos the functions $R(r)$ and $H(r)$ take the form

$$R(r) = \sinh r \cosh r \quad (2.2a)$$

$$H(r) = \sqrt{2} \sinh^2 r \quad (2.2b)$$

where $a^2 = 4/\omega^2$ and ω is a measure of the constant rotation of the matter flow of the model. Coordinates t , r and ϕ are defined on a 3-dim hyperboloid H^3 (up to identification of certain point sets), [1,4,5] with range $-\infty < t < \infty$, $0 \leq r < \infty$, $0 \leq \phi \leq 2\pi$. The coordinate z is defined on the real line R . The manifold of the model has structure of $H^3 \times R$ (up to identification of certain points) and is completely covered by the above coordinate system.

The geodesic equations of motion are expressed

$$V^\mu \parallel V^\nu = 0 \quad (2.3)$$

where $V^\mu = (\dot{t}, \dot{r}, \dot{\phi}, \dot{z})$ is the vector field tangent to the curve parametrized with parameter s , and where a dot denotes derivative with respect to s . Equations (3) have the set of independent first integrals

$$\dot{t} + H \dot{\phi} = A_0 \quad (2.4a)$$

$$(H^2 - R^2) \dot{\phi} + H \dot{t} = B_0 \quad (2.4b)$$

$$\dot{t}[\dot{t} + H\dot{\phi}] + \dot{\phi}[H\dot{t} + (H^2 - R^2)\dot{\phi}] - \dot{r}^2 = \frac{\epsilon}{a^2} + C_0^2 \quad (2.4c)$$

$$\dot{z} = C_0 \quad (2.4d)$$

where A_0 , B_0 and C_0 are integration constants and $\epsilon = 1, 0$ accordingly if the geodesics is time-like or null, respectively. For Gödel's geometry these equations reduce to

$$\dot{t} + \sqrt{2} \sinh^2 r \dot{\phi} = A_0 \quad (2.5a)$$

$$\sqrt{2} \sinh^2 r \dot{t} + (\sinh^4 r - \sinh^2 r) \dot{\phi} = B_0 \quad (2.5b)$$

$$\dot{z} = C_0 \quad (2.5c)$$

$$\dot{r}^2 = \dot{t}^2 + 2\sqrt{2} \sinh^2 r \dot{t}\dot{\phi} + (\sinh^4 r - \sinh^2 r) \dot{\phi}^2 - (C_0^2 + \epsilon/a^2) \quad (2.5d)$$

From a direct inspection of equations (2.3) we single out

the two families of geodesics characterized by

$$V^\mu = \lambda(1, 0, 0, 1 - \frac{1}{\lambda}) \quad (2.6a)$$

$$V^\mu = \lambda(1, 0, 0, 1) \quad (2.6b)$$

respectively time-like and null-like curves, in which λ is a positive arbitrary number. For $\lambda=1$ the congruence determined by (2.6a) are the world lines of the matter content of the model. The set (2.5), (2.6) exhausts all possible solutions of the equation of geodesics.

We can rewrite equations (2.5) as

$$\dot{\phi} = \frac{\sqrt{2} A_0}{\cosh^2 r} - \frac{B_0}{\sinh^2 r \cosh^2 r} \quad (2.7a)$$

$$\dot{t} = A_0 \left[1 - \frac{2 \sinh^2 r}{\cosh^2 r} \right] + \frac{\sqrt{2} B_0}{\cosh^2 r} \quad (2.7b)$$

$$\dot{z} = C_0 \quad (2.7c)$$

$$\dot{r}^2 = A_0^2 - D_0^2 - \left(\sqrt{2} A_0 \frac{\sinh r}{\cosh r} - \frac{B_0}{\sinh r \cosh r} \right)^2 \quad (2.7d)$$

Although equations (2.7) can be directly integrated (a task which we postpone for section 5) let us investigate here the general behaviour of the geodesic families by using the powerful method of the *Effective Potential*. This allows us to obtain directly many results of section 5 and also gives us a deeper insight on the global properties of motion in Gödel's space-time.

III. THE EFFECTIVE POTENTIAL

Equation (2.7d) can be expressed

$$\dot{r}^2 = A_0^2 - V(r) \quad (3.1)$$

where the effective potential $V(r)$ has the form

$$V(r) = \left[\sqrt{2} A_0 \frac{\sinh r}{\cosh r} - \frac{B_0}{\sinh r \cosh r} \right]^2 + D_0^2 \quad (3.2)$$

Here we denote

$$D_0^2 = C_0^2 + \epsilon/a^2 \quad (3.3)$$

From the above equations we can easily see that A_0^2 is the square of the total energy in case of photons (null curves, $\epsilon=0$) and the square of the total energy per unit of mass for massive particles (time-like curves, $\epsilon = 1$). Also B_0 is interpreted as the total angular-momentum of the trajectories. In fact, introducing the momenta $p_\mu = g_{\mu\nu} \dot{x}^\nu$ we have $p_0 = A_0$, $P_r = -\dot{r}$, $P_\phi = B_0$, $P_z = -C_0$, and equation (2.7d) can be put into the form $p_0^2 = p_r^2 + p_z^2 + \frac{(p_\phi - a(r))^2}{R^2} + \epsilon/a^2$. R is given by (2.2a) and we note that this expression is analogous to the equation of a charged particle in the presence of the vector potential $A_\phi = a(r)$. In what follows we shall briefly refer to A_0 as the "energy" of the particles (geodesic trajectories).

Now using equation (3.1) we can make a complete characterization of the motion into three distinct cases: $B_0 > 0$, $B_0 = 0$ and $B_0 < 0$, as the corresponding potentials $V(r)$ are basically dis-

tinct. Let us define the parameters

$$\gamma = B_0/A_0 \quad \beta^2 = D_0^2/A_0^2 \quad (3.4)$$

For physical particles we must have $0 \leq \beta^2 \leq 1$. The potential $V(r)$ is depicted in Figs. 1a, b, c. We have actually plotted $V(r) - \beta^2 A_0^2$ and, in the case of $\beta^2 = 0$, the graphs represent $V(r)$ directly. For $\beta^2 \neq 0$, $V(r)$ is obtained by an upward shift of the graphs.

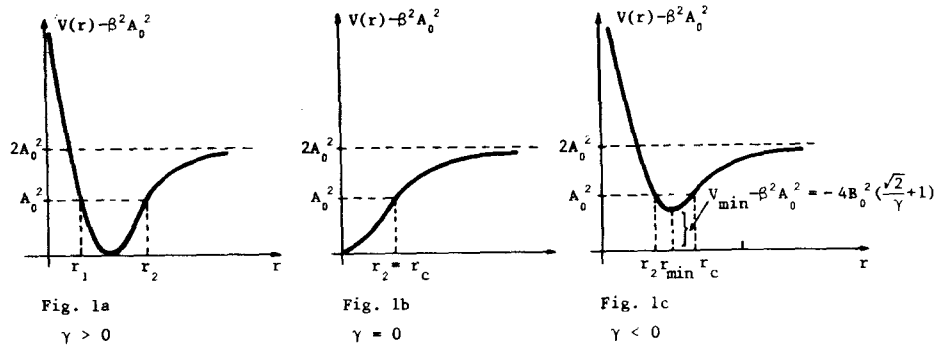


FIGURE 1: Graphs of the Effective Potential

Let us discuss the three distinct cases of the above figures. The radial coordinate r oscillates in the allowable classical domain $r_1 \leq r \leq r_2$, the turning points being

$$\sinh^2 r_i = \frac{1 + 2\sqrt{2}\gamma - \beta^2 \pm \sqrt{1 - \beta^2} \sqrt{(2\gamma + \sqrt{2})^2 - (1 + \beta^2)}}{2(1 + \beta^2)} \quad (3.5)$$

respectively for $i = 1, 2$, and for which $\dot{r}^2 = 0$ (equivalently $V(r) = A_0^2$). Since the total "energy" A_0^2 is a fixed quantity for each geodesic the trajectory is kept within the cylindrical shell $r_1 \leq r \leq r_2$. We show later that the trajectories are closed in the (r, ϕ) -plane. We now consider

Case 1: $\gamma > 0$

The case $\beta^2=0$ corresponds to photon trajectories in a $z = \text{const.}$ plane. For massive particles or photons with non-null momentum along z ($\beta^2 \neq 0$) the width of the cylindrical shell diminishes and goes to zero for $\beta^2=1$. Indeed this limit $\beta^2=1$ corresponds to an upward shift of A_0^2 for the potential of Fig. 1 — the new minimum of the curve $V(r)$ is now equal to A_0^2 . This implies that the width of the shell is zero, localizing the r -coordinate of the particle at $r = r_{\min} = \text{arc sinh}^2 \frac{\sqrt{2}}{2} \gamma$.

On the other hand the value of r corresponding to the minimum of the potential ($\text{sinh}^2 r = \frac{\sqrt{2}}{2} \gamma$) makes $\dot{\phi} = 0$ (cf. eq.(2.7a)) for any $\beta^2 \leq 1$. This is actually a necessary condition for the motion of the particle to occur inside the cylindrical shell, as this guarantees that the extremum $\dot{\phi} = 0$ always occur inside the shell. For $\beta^2=1$ we have $\dot{\phi}=0$ always, and the particle moves only in the z -direction, which corresponds to the solutions (2.6 a,b) for $\varepsilon = 1,0$ respectively.

Finally we should notice that from the dependence of r_i on the parameter γ , we can see that the cylindrical shell can be located at any distance from the axis $r=0$, for different values of γ . We remark also that geodesics with $\gamma > 0$ are not allowed to reach the origin $r=0$. The form of the potential is highly stable with respect to variations of the total "energy" A_0^2 of the particles, and as a consequence its properties are valid for all finite values of A_0^2 .

IV. CONFINEMENT

We now show that for $\gamma \leq 0$ the potential $V(r)$ produces a confinement of all the trajectories within the cylinder $r \leq r_c$, with $\sinh r_c = 1$.

Case 2: $\gamma = 0$

For $\beta^2 = 0$ it is remarkable that the maximum radial distance which any of these ($\gamma=0$) photons can attain is given by $\sinh r_c = 1$. This fact was also noticed in Ref. [2]. Remarkably enough this value $r = r_c$ has been defined by Gödel as a limiting value separating causal from acausal regions of the space-time. In fact, the form of the potential $V(r)$ given in Fig. 1b shows that for any value of the total energy A_0^2 the photons are always confined inside the cylindrical surface $r = r_c$. But we see that this result holds also for massive particles although they are never able to attain the limiting wall.

Case 3: $\gamma < 0$

From equations (3.2) we obtain that $V(r)$ has a minimum (cf. Fig. 1c) at

$$r_{\min} = \text{arc sinh}^2 \frac{-\frac{\sqrt{2}}{2}\gamma}{1+\sqrt{2}\gamma} \quad (3.6)$$

Contrary to the two previous cases the minimum of $V - \beta^2 A_0^2$ is not zero but has the non-null value $V_{\min} - \beta^2 A_0^2 = -4B_0^2 \left(\frac{\sqrt{2}}{\gamma} + 1 \right)$. However from equation (3.1) we must have

$$V_{\min} \leq A_0^2 \quad (3.7)$$

This implies that the permissible range of negative values of γ is bounded [6],

$$\frac{-\sqrt{2} + \sqrt{1+\beta^2}}{2} \leq \gamma < 0, \quad (3.8)$$

the lower bound $\gamma = \gamma_{\min} = \frac{-\sqrt{2} + \sqrt{1+\beta^2}}{2}$ corresponding to the equality in (3.7). Contrary to the two previous cases, in which $V_{\min} = A_0^2$ is equivalent to $\beta^2=1$, $\dot{\phi}=0$ — the limiting situation $V_{\min} = A_0^2$ leads to values $\beta^2 < 1$ and $\dot{\phi} \neq 0$. Thus in this limit the orbits will have $r = r_{\min} = \text{const.}$ with $\gamma = \gamma_{\min}$ and $\dot{\phi} = \text{const} \neq 0$. These are circular orbits (more precisely the projection of the orbits in the plane (r, ϕ) are circular) and it is clear that the only possible case of circular orbits corresponds exactly to the lower bound of γ .

We remark that for any case the allowable range of γ is given by

$$\frac{-\sqrt{2} + \sqrt{1+\beta^2}}{2} \leq \gamma < \infty \quad (3.9)$$

By substitution of the value $\gamma_{\min} = \frac{-\sqrt{2} + \sqrt{1+\beta^2}}{2}$ in (3.6) we obtain the radius of the circular orbits given by

$$\sinh^2 r = \frac{\sqrt{2} - \sqrt{1+\beta^2}}{2\sqrt{1+\beta^2}} \quad \text{or} \quad \cosh 2r = \frac{\sqrt{2}}{\sqrt{1+\beta^2}} \quad (3.10)$$

and (2.7a) and (3.10) give $\dot{\phi} = 2 A_0 \sqrt{1+\beta^2}$. From (3.10) we find that for all circular orbits $r \leq \frac{1}{2} \text{arc cosh } \sqrt{2} < r_c$, the maximum radius corresponding to a null geodesics, as pointed out in Ref. [3]. We find also that for $\gamma < 0$, $\dot{\phi} > 0$ always, that is, $\dot{\phi}$ cannot change sign along these trajectories. More general

ly from (3.4) we see that $r_2 < r_c$ for $\gamma < 0$, which confirms our previous statement that all orbits with $\gamma \leq 0$ are confined inside the cylinder $r = r_c$. In other words, the gravitational field of Gödel's cosmos selects a whole class of particles (photons or massive particles, with $\gamma \leq 0$) and isolate them inside the region $r \leq r_c$.

V. THE INTEGRATION OF GEODESICS EQUATIONS

To obtain more information about the geodesic motion in Gödel's universe, let us now integrate completely the system of equations (2.7).

Equation (2.7c) can be immediately integrated to

$$z = C_0 s + z_0 \quad (5.1)$$

To integrate equation (2.7d) or (3.1) we introduce the variable ρ defined by

$$\rho = \sinh^2 r \quad (5.2)$$

Equation (3.1) is then reexpressed

$$\dot{\rho}^2 = 4 A_0^2 \{ -(1+\beta^2) \rho^2 + (1+2\sqrt{2}\gamma-\beta^2) \rho - \beta^2 \} \quad (5.3)$$

a solution of which is given by

$$\rho(s) = \frac{1+2\sqrt{2}\gamma-\beta^2}{2(1+\beta^2)} + \frac{\sqrt{1-\beta^2}}{2(1+\beta^2)} \sqrt{(2\gamma+\sqrt{2})^2 - (1+\beta^2)} \cos 2 A_0 \sqrt{1+\beta^2} (s-s_0) \quad (5.4)$$

This solution corresponds to have chosen s_0 such that ρ is maximum at $s = s_0$.

We reobtain now a number of results which have been obtained in section III from equation (3.5) and the analysis of Figs. 1a, b, c, showing the power of the method of the Effective Potential. The values of ρ_{\max} and ρ_{\min} drawn from (5.4) are obviously the roots r_i given in (3.5), namely

$$\rho_{\max}^{\min} = \frac{1 + 2\sqrt{2}\gamma - \beta^2 \pm \sqrt{1-\beta^2} \sqrt{(2\gamma+\sqrt{2})^2 - (1+\beta^2)}}{2(1+\beta^2)} \quad (3.5)$$

From (3.5) or (5.4) we must have

$$(2\gamma+\sqrt{2})^2 \geq (1+\beta^2) \quad (5.5)$$

This inequality together with the obvious condition $\rho \geq 0$ implies (cf. Ref. [6])

$$\frac{-\sqrt{2} + \sqrt{1+\beta^2}}{2} \leq \gamma < \infty, \quad (3.9)$$

the lower limit corresponding to the equality in (5.5).

We also have that ρ is a constant for the cases

$$(i) \quad \beta^2 = 1$$

$$(ii) \quad \gamma = \frac{-\sqrt{2} + \sqrt{1+\beta^2}}{2},$$

from (3.5) taking $\rho_{\max} = \rho_{\min}$, or from (5.4). Case (i) gives $\rho = \frac{\sqrt{2}}{2} \gamma$ which implies $\dot{\phi} = 0$. These are curves with $\rho, \phi = \text{const.}$, and a velocity vector field along the z-axis. Case (ii)

corresponds to the lower limit of γ (cf. (3.9)) and we have

$$\rho = \frac{\sqrt{2} - \sqrt{1+\beta^2}}{2\sqrt{1+\beta^2}} \quad (3.10)$$

or, equivalently,

$$\cos 2r = \frac{\sqrt{2}}{\sqrt{1+\beta^2}}$$

which for $0 \leq \beta^2 \leq 1$ implies $1 \leq \cosh 2r \leq \sqrt{2}$, as already mentioned. Also $\dot{\phi} = \text{const} = 2 A_0 \sqrt{1+\beta^2}$ and it is clear that this is the case of "circular" orbits (actually spatial helices if $C_0^2 \neq 0$).

We also remark that for both cases (i) and (ii) the orbits $r = \text{const.}$ are stable, since they are located at the minimum of the potential $\ddot{r} = -\frac{dV}{dr} = 0$.

Of course all the above results are contained in equation (5.4), which shall be used in what follows. We now turn to the integration of $\phi(s)$. Our choice of solution (5.4) corresponds to take for equation (5.3) the root

$$\dot{\rho} = -2 A_0 \sqrt{-(1+\beta^2)\rho^2 + (1+2\sqrt{2}\gamma-\beta^2)\rho - \beta^2} \quad (5.6)$$

Using (2.7a),

$$\dot{\phi} = A_0 \frac{\sqrt{2}\rho - \gamma}{\rho(\rho+1)} \quad (2.7a)$$

we have

$$\frac{d\phi}{d\rho} = \frac{-(\sqrt{2}\rho - \gamma)}{2\rho(\rho+1) \sqrt{-(2\rho - \gamma)^2 + (1+\beta^2)\rho(\rho+1)}}$$

which can be immediately integrated to

$$2(\phi - \phi_0) = A + B \quad (5.7)$$

where ϕ_0 is an integration constant, and

$$A = \arcsin \frac{(1 - \beta^2 + 2\sqrt{2}\gamma) \rho - 2\gamma^2}{\rho \sqrt{1 - \beta^2} \sqrt{(2\gamma + \sqrt{2})^2 - (1 + \beta^2)}} \quad (5.8)$$

$$B = \arcsin \frac{[2\gamma(\sqrt{2} + \gamma) + 1 - \beta^2](\rho + 1) - 2(\sqrt{2} + \gamma)^2 \rho}{(\rho + 1) \sqrt{1 - \beta^2} \sqrt{(2\gamma + \sqrt{2})^2 - (1 + \beta^2)}} \quad (5.9)$$

Equation (5.7) results

$$\cos(\phi - \phi_0) = \frac{(2\gamma + \sqrt{2}) \rho + \gamma}{\sqrt{(2\gamma + \sqrt{2})^2 - (1 + \beta^2)} \sqrt{\rho(\rho + 1)}} \quad (5.10)$$

for $\cos A \cos B < 0$. The case $\cos A \cos B > 0$ is compatible only for $\gamma = 0$ in which case the solution coincides with (5.10). From (5.10) and (5.4) we can easily conclude that the trajectories are closed in the (ρ, ϕ) - plane. We remark that the expression (5.10) is not valid for the orbits with $\rho = \text{const.}$ (cases (i) and (ii) above).

The equation for $t(s)$ can also be integrated to

$$\text{tg} \frac{\sqrt{2}}{2} (t + A_0 (s - s_0)) = \frac{1 + \beta^2 + \sqrt{2}(2\gamma + \sqrt{2}) - \sqrt{1 - \beta^2} \sqrt{(2\gamma + \sqrt{2})^2 - (1 + \beta^2)}}{2(\gamma + \sqrt{2}) \sqrt{1 + \beta^2}} \text{tg} A_0 \sqrt{1 + \beta^2} (s - s_0) \quad (5.11)$$

For the two limit cases (i) $\beta^2 = 1$ and (ii) $\gamma = \frac{-\sqrt{2} + \sqrt{1 + \beta^2}}{2}$, expression (5.11) can be simplified and yields

$$(i) \ t = A_0 (s - s_0) \quad , \quad (ii) \ \frac{\sqrt{2}}{2} t = A_0 \left(\sqrt{1 + \beta^2} - \frac{\sqrt{2}}{2} \right) (s - s_0)$$

An alternative expression to calculate $t(s)$ is obtained by noting that — for a given geodesics characterized by A_0 , B_0 , C_0 — we have

$$A_0 t(s) - F(r(s)) + B_0 \phi(s) - C_0 z(s) - \epsilon(s-s_0) = 0 \quad (5.12)$$

where $F(r) = \int dr \sqrt{A_0^2 - V(r)}$, which is an obvious integral of $p_\mu V^\mu = \epsilon$. We remind that $\epsilon = 1, 0$ for time-like and null-like geodesics respectively.

VI GRAPHS OF TRAJECTORIES IN THE (ρ, ϕ) - PLANE

With the aid of the results of the previous sections we can now have a general picture of the projection of geodesic trajectories of particles on the (ρ, ϕ) - plane. From expression (5.10) it follows that [7].

$$\cos(\phi - \phi_0) = \pm 1 \quad (6.1)$$

for $\rho = \rho_{\max, \min}$ (cf. (3.5)). More specifically

$$\text{if } \gamma > 0: \quad \cos(\phi - \phi_0) = +1 \quad \text{for } \rho_{\max}, \rho_{\min} \quad (6.2)$$

$$\text{if } \gamma < 0: \quad \cos(\phi - \phi_0) = +1 \quad \text{for } \rho_{\max} \quad (6.3)$$

$$\cos(\phi - \phi_0) = -1 \quad \text{for } \rho_{\min}$$

By the other hand, expression (2.7a) defines the value

$$\rho_\phi = \frac{\sqrt{2}}{2} \gamma \quad (6.4)$$

and that $\dot{\phi}|_{\rho=\rho_{\phi}} = 0$. We also note that $\dot{\phi} > 0$ at $\rho = \rho_{\max}$. It results

$$\text{if } \gamma > 0: \quad \rho_{\min} < \rho_{\phi} < \rho_{\max} \quad (6.5)$$

$$\text{if } \gamma < 0: \quad \rho_{\min} < \rho_{\max} \quad (6.6)$$

$$\dot{\phi} > 0 \text{ always}$$

$$\text{if } \gamma = 0: \quad \rho_{\min} = 0 \quad (6.7)$$

$$\rho_{\max} = \frac{1-\beta^2}{1+\beta^2}$$

We remind once more that for $\gamma = \frac{-\sqrt{2} + \sqrt{1+\beta^2}}{2}$ (the lower limit of γ values) we have "circular" orbits with $\rho = \frac{\sqrt{2} - \sqrt{1+\beta^2}}{2\sqrt{1+\beta^2}}$. The graphs of Fig.2 are illustrative.

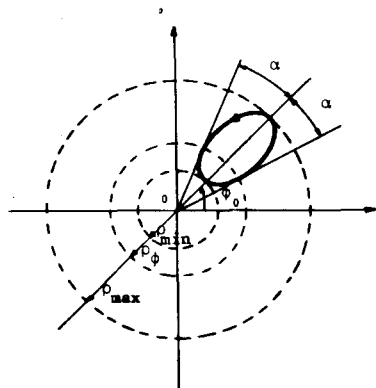


Fig. 2a: $\gamma > 0$

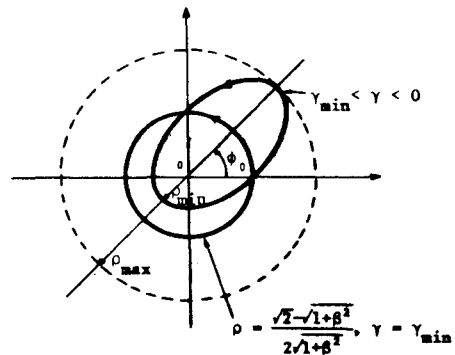


Fig. 2b: $\gamma < 0$

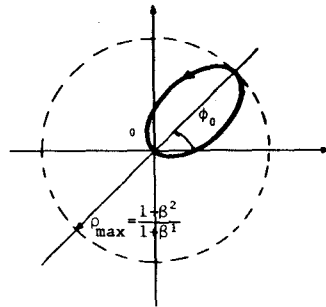


Fig. 2c: $\gamma = 0$

FIGURE 2: Graphs of geodesic trajectories in (ρ, ϕ) -plane

As γ becomes large

$$\rho_{\max} - \rho_{\min} \rightarrow \frac{2\sqrt{1-\beta^2}}{1+\beta^2} \gamma \quad (6.8)$$

and

$$\frac{1}{2}(\rho_{\max} + \rho_{\min}) \rightarrow \frac{\sqrt{2}\gamma}{1+\beta^2}, \quad \alpha \rightarrow \frac{\sqrt{1+\beta^2}}{2\gamma} \quad (6.9)$$

In other words, as $\gamma \rightarrow \infty$ the angle goes to zero and the ellipse of Fig. 2a is located at an infinite distance from the origin (cf. (6.9)). From (6.8) we have to distinguish three cases: (i) for fixed β^2 , as $\gamma \rightarrow \infty$ the ellipse is stretched infinitely along the direction $\phi = \phi_0$; (ii) if γ increases as $\frac{k_0}{\sqrt{1-\beta^2}}$ for $\beta^2 \rightarrow 1$, the ellipse is stretched along the direction $\phi = \phi_0$ in an interval of length k_0 ; (iii) if γ increases as $\frac{1}{(1-\beta^2)^{k/2}}$ for $\beta^2 \rightarrow 1$, where $k > 1$, the ellipse reduces to a point at an infinite distance of $r = 0$ along the direction $\phi = \phi_0$.

We depict several curves for increasing γ , in Fig. 3. We remark that the trajectories have all the same counter clockwise direction.

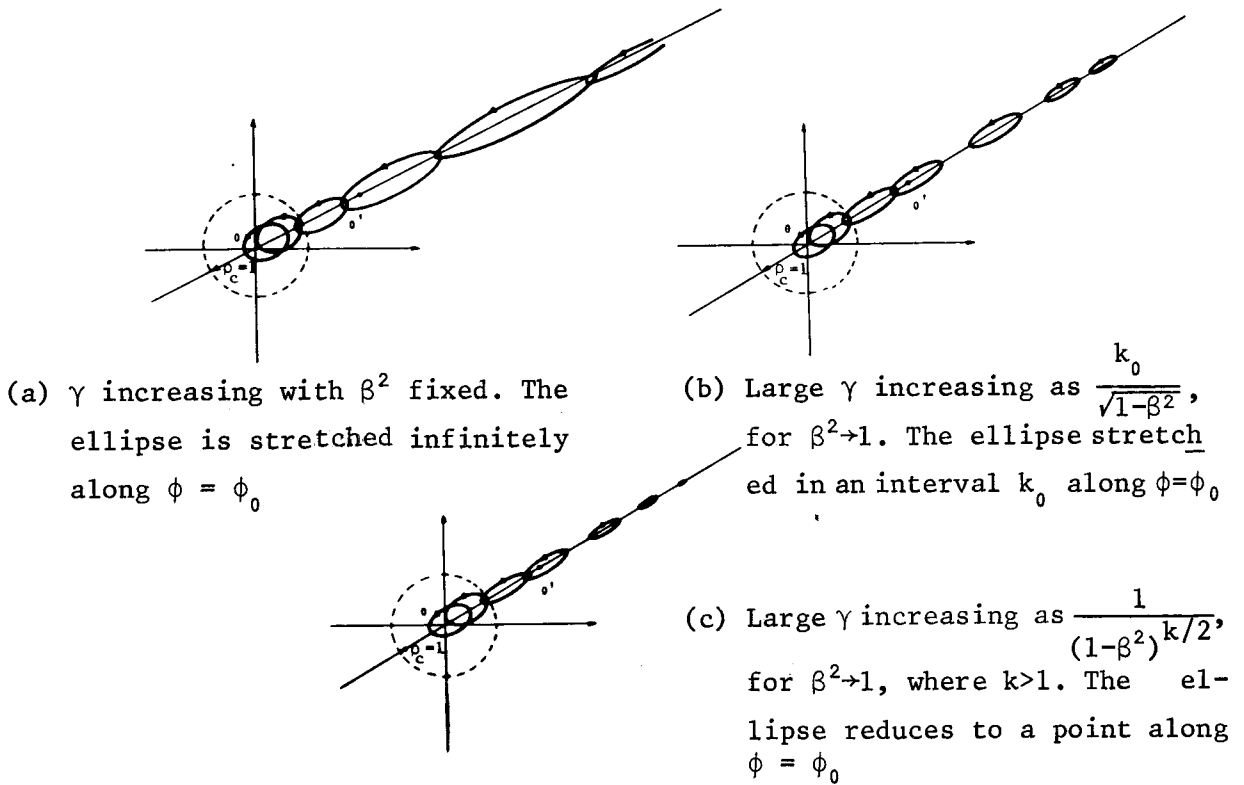


FIGURE 3: Graphs of the (ρ, ϕ) -trajectories for increasing γ

VII HOMOGENEITY IN SPACE-TIME - TRAVEL BACK IN TIME

From the above picture we can now make a comment about the homogeneity properties of free motion in Gödel's universe. It is suggestive that the structure of curves that occurs around $r = 0$ is reproduced at any point $r \neq 0$, up to a suitable deformation which comes from the r -dependence of the metric coefficients. In other words, the structure of geodesics about the origin 0 is topologically equivalent to the structure about any other point $0'$. Indeed we now know that the properties of the

curves depend basically on the value of the angular-momentum parameter γ of the trajectory, relative to the origin $r = 0$, and in principle it is always possible to find a new parameter γ' — connected to the origin $0'$ of a new coordinate system — such that one set of the old elliptic curves can be circular orbits around the new origin and vice-versa. In this way, the structure of the potentials of Figs 1a, b and c as well the structure of curves of Figs. 2a, b and c about the origin $r = 0$ are reproduced for each observer taken as defining the new origin $0'$ of the coordinate system (see Fig.3). This observer (located at the origin $r = 0$ of a given coordinate system) will nevertheless be constrained to see only the portion of the universe inside the cylinder $r = r_c$, because all geodesics which can reach $r = 0$ are confined inside the cylinder $r = r_c$.

Beyond $\rho = \rho_c = 1$ (that is, $r = r_c$) it occurs the fact that the time coordinate t runs backwards. This can be seen from the expression (2.7b),

$$\dot{t} = A_0 \frac{(\sqrt{2}\gamma + 1) - \rho}{\rho + 1} \quad (2.7b)$$

that defines the value of ρ

$$\rho_t = \sqrt{2}\gamma + 1 \quad (7.1)$$

for which $\dot{t} = 0$. For $\rho > \rho_t$ we see from (2.7b) that t decreases. From (7.1) and the allowable range of γ (cf.(3.9)) we can verify that for $\gamma_{\min} < \gamma < 0$, $\rho_{\max} < \rho_t$. The first

root of the equation $\rho_{\max} = \rho_t$ occurs for $(\gamma = 0, \beta^2 = 0)$. The diagrams of Fig.4 are illustrative of the properties of the curves for several γ , with respect to ρ_t and ρ_c .

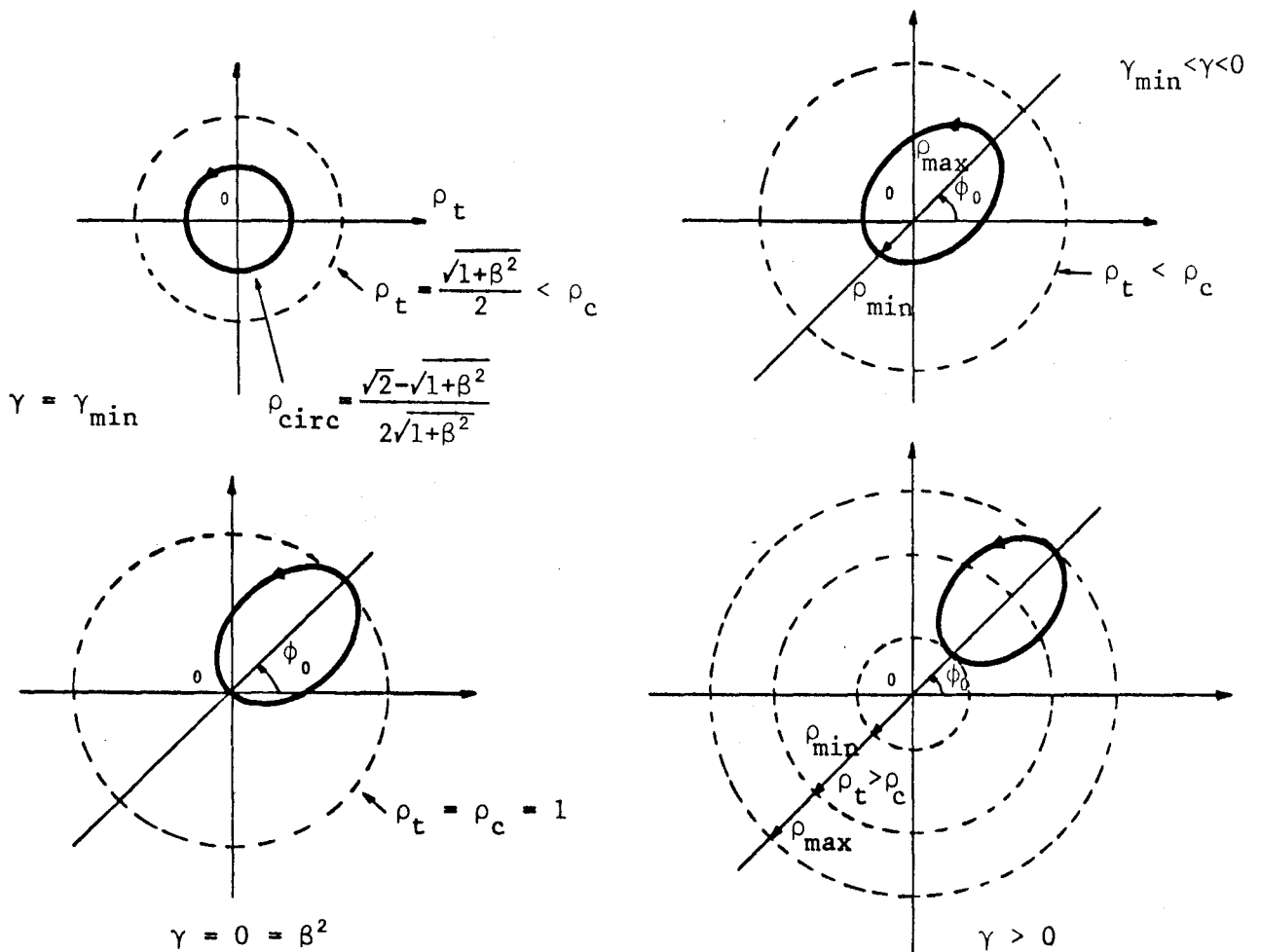


FIGURE 4: Graphs of the trajectories in the (ρ, ϕ) -plane for several values of γ , with respect to ρ_c (Gödel's critical radius $\rho_c = \sinh^2 r = 1$) and ρ_t (for values of ρ beyond ρ_t the time-coordinate t decreases).

VIII CONCLUSIONS

Although the study of geodesics in Gödel's universe has been undertaken more than twenty years ago by Kundt, and Chandrasekhar and Wright^[2,3], the complete physical features of geodesic motion in this geometry remained somewhat obscure, possibly related to the choice of the coordinate system used by these authors to integrate the geodesic equations. In the past twenty years, there seemed to be a general inability to recognize that the direct use of cylindrical coordinates allows a deeper insight into the properties of geodesics and that in this coordinate system we are able to use in a very powerful way the method of the Effective Potential. Also in this coordinate system (t,r,ϕ,z) the first integrals of motion (velocity component along the z -axis, energy, and angular-momentum with respect to the origin $r=0$) provide a simpler and more physical parametrization of the equations of motion. The Effective Potential is completely characterized by this set of physical constants of motion, and its form is highly stable under variation of these parameters. In particular the ratio γ of the angular-momentum with respect to the origin to the energy of the orbit allows us to distinguish three families of geodesics, whether respectively $\gamma>0$, $\gamma=0$ and $\gamma<0$. The negative range of γ is limited, the lower bound corresponding to the family of circular orbits in the (r,ϕ) -plane. The important property of confinement of geodesics is produced by Gödel's geometry: from the graphs of the potential we obviously see (cf. Fig.1) that all geodesics for $\gamma\leq 0$ are confined inside the cylinder $r=r_c$ about the origin, where r_c is Gödel's crit

ical radius $[1]$. The only geodesics which can reach the limiting wall $r=r_c$ are photon trajectories with zero velocity along the z -axis. This confinement is independent of the energy of the particles. In other words an ensemble of particles with $\gamma \leq 0$ is always confined inside the cylinder with radius r_c about the origin $r=0$, for any distribution of the particles energy.

The above results are obtained directly from the explicit expression of the Effective Potential. From further investigation of geodesic equations we show that, except for one limiting case, all trajectories are closed curves in the (r, ϕ) -plane. For $\gamma < 0$, the origin $r=0$ is contained inside the curve, for $\gamma > 0$ the origin is outside and only for $\gamma = 0$ the curve passes through the origin. All trajectories have the same counterclockwise direction about any point contained inside the curve in the (r, ϕ) -plane. In this sense we say that all trajectories co-rotate with the matter content of the model. For large values of γ ($\gamma \rightarrow \infty$) the trajectories are located at an infinite distance from the origin $r=0$ and their behaviour at infinity depends on the asymptotic behaviour of γ (cf. Fig 3) with respect to the ratio $(p_z^2 + \epsilon/a^2)/p_0^2$.

The structure of the curves about the origin of the coordinate system is reproduced about any point $0'$, up to a suitable deformation, that is, the structure of geodesics about the origin 0 is topologically equivalent to the structure about any other point $0'$. The latter could be described in the same way by a new parameter γ' associated to the angular momentum of the orbits about $0'$, as should be expected from the homogeneity of the space-time.

The fact that the time coordinate t decreases occurs only beyond $r=r_c$, along geodesics with $\gamma>0$. This does not represent a direct violation of causality with geodesics.

We now use the confinement property of Gödel's geometry to discuss the construction of an idealized gravitational container. As we have mentioned earlier the topology of Gödel's manifold is $H^3 \times R$, with the z -coordinate defined on the real line R . We are then free to identify certain point sets in R , changing the topology into $H^3 \times S^1$ and generating a new universe locally isometric to Gödel's cosmos [9]. The surface $r=r_c$ is then transformed into the compact surface of a torus and all trajectories of $\gamma \leq 0$ particles are contained in the interior of this torus surface, for any distribution of energy of the particles. This ensemble of particles constitute a structure whose gravitational stability is guaranteed by the inexistence of singularities in the interior of the surface $r=r_c$. No other gravitational field seems to produce this type of stable structure. We can then speculate if in the actual universe gravitation could produce, through inhomogeneous matter rotation, a sample of these idealized containers hiding in its interior an unexpected source of energy.

APPENDIX

For completeness and future reference we give here the relation between our constants of motion and the constants which appear in Ref. [3].

Expression (46) of Ref. [3],

$$\cosh 2r = \frac{1 + e^{2c_1} (\cos^2 \sigma + 2 \sin^2 \sigma)^2 + \frac{(\alpha-1)^2}{4\alpha} \sin^2 2\sigma}{2e^{c_1} (\cos^2 \sigma + \alpha \sin^2 \sigma)}$$

can be simplified to

$$\cosh 2r = Q + P \cos 2\sigma \quad (A1)$$

where

$$P = \left(\frac{1-\alpha}{4}\right) (e^{c_1} - e^{-c_1/\alpha}) \quad (A2)$$

$$Q = \left(\frac{1+\alpha}{4}\right) (e^{c_1} + e^{-c_1/\alpha}) \quad (A3)$$

Introducing a new parameter χ such that [8]

$$\alpha = e^{-\chi} \quad (A4)$$

P and Q can be expressed

$$P = \sinh \chi/2 \sinh(c_1 - \chi/2) \quad (A5)$$

$$Q = \cosh \chi/2 \cosh(c_1 - \chi/2) \quad (A6)$$

With respect to our constants of motion, the parameter σ is

given by

$$\sigma = A_0 \sqrt{1+\beta^2} (s-s_0) \quad (A7)$$

for our choice of the origin $s = s_0$ corresponding to $\rho = \rho_{\max}$ (cf. (5.4)).

Now comparing (5.4) with (A1), and using expressions (A5) - (A7) we obtain the desired relations

$$\sinh^2 \chi/2 = \frac{1-\beta^2}{1+\beta^2}, \quad \cosh^2 \chi/2 = \frac{2}{1+\beta^2} \quad (A8)$$

$$\sinh^2(c_1 - \chi/2) = \frac{(2\gamma + \sqrt{2})^2 - (1+\beta^2)}{1+\beta^2}, \quad \cosh^2(c_1 - \chi/2) = \frac{(2\gamma + \sqrt{2})^2}{1+\beta^2} \quad (A9)$$

We note that for $\gamma = \gamma_{\min}$ (cf. (3.9)), $\cosh^2(c_1 - \chi/2) = 1$.

Also from our expressions (5.4), (5.6) and (5.10) we obtain straightforwardly equation (45) of Ref. [2]. In fact expressing (5.4) as $\rho = Q' + P' \cos 2\sigma$ and using the result of Ref. [7], we can rewrite (5.10) as

$$2\sqrt{\rho(\rho+1)} \cos(\phi - \phi_0) = \sqrt{4\rho(\rho+1) - \left(\frac{1-\beta^2}{1+\beta^2}\right) + \left(\frac{1-\beta^2}{1+\beta^2}\right) \left(\frac{\rho-Q'}{P'}\right)^2}$$

and it follows then

$$4\rho(\rho+1) \sin^2(\phi - \phi_0) = \left(\frac{1-\beta^2}{1+\beta^2}\right) \left[1 - \left(\frac{\rho-Q'}{P'}\right)^2\right] = \left(\frac{1-\beta^2}{1+\beta^2}\right) \sin^2 2\sigma$$

or

$$2\sqrt{\rho(\rho+1)} \sin(\phi - \phi_0) = \sqrt{\frac{1-\beta^2}{1+\beta^2}} \sin 2\sigma$$

which, using the relation (A8), reproduces equation (45) of Ref. [3].

REFERENCES

- [1] K. Gödel, Rev. Mod. Phys. 21, 447 (1949)
- [2] W. Kundt, Z. Phys. 145, 611 (1956). We become aware of Kundt's results through J. Pfarr GRG 13, 1073 (1981)
- [3] S. Chandrasekhar and J.P. Wright, Proc. Nat. Acad. Sci. 47, 341 (1961)
- [4] I. Ozsvath, J. Math. Phys. 11, 2871 (1970)
- [5] I. Damião Soares and L.M.C.S. Rodrigues, Proc, of the IIIrd Brazilian Summer School of Cosmology and Gravitation (Rio de Janeiro, 1982)
- [6] Inequality (3.7) for negative γ is satisfied for values of γ given by

$$(i) \frac{-\sqrt{2} + \sqrt{1+\beta^2}}{2} \leq \gamma < 0$$

$$(ii) \gamma \leq -\frac{\sqrt{2} + \sqrt{1+\beta^2}}{2}$$

The domain (ii) is excluded because $\sin^2 r_{\min}$ is negative for these values.

- [7] The following result is useful for deriving (5.13)

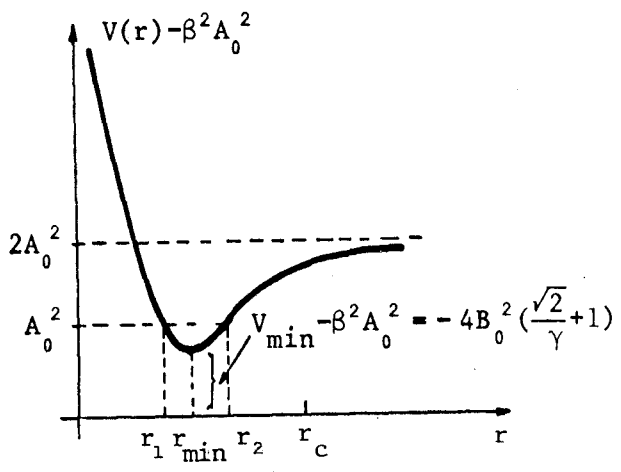
$$[(2\gamma+\sqrt{2})\rho+\gamma]^2 = \left[\frac{(2\gamma+\sqrt{2})^2 - (1+\beta^2)}{4} \right] \cdot \left\{ 4 \rho(\rho+1) - \left(\frac{1-\beta^2}{1+\beta^2} \right) + \left(\frac{1-\beta^2}{1+\beta^2} \right) \left(\frac{\rho-Q}{P} \right)^2 \right\}$$

where P and Q are given from expression (5.4) rewritten as

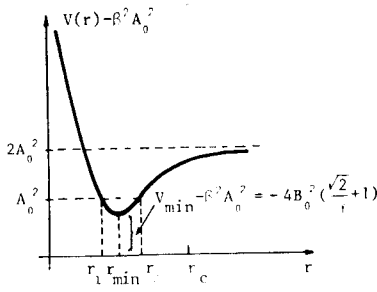
$$\rho(s) = Q + P \cos 2 A_0 \sqrt{1+\beta^2} (s-s_0).$$

- [8] Since $(\sqrt{2}-1)^2 \leq \alpha \leq 1$ we have $0 \leq \chi \leq -2\ell n(\sqrt{2}-1)$
- [9] It is important to note that the new manifold $H^3 \times S^1$ also has the structure of a Lie group. A curve globally defined in $H^3 \times R$ is then globally defined in $H^3 \times S^1$.

ERRATA

Page	Line	In place of	Read
5	18	A_0	A_0^2
6	-	Fig. 1c	 <p style="text-align: center;">Fig. 1c $\gamma < 0$</p>
8	10 21	a causal is not	acausal is never
12	4	$\cos 2r$	$\cosh 2r$
15	1	and	such
21	23	situable	suitable
25	3	become	became

ERRATA

Page	Line	In place of	Read
5	18	A_0	A_0^2
6	-	Fig. 1c	 <p style="text-align: center;">Fig. 1c $\gamma < 0$</p>
8	10 21	a causal is not	acausal is never
12	4	$\cos 2r$	$\cosh 2r$
15	1	and	such
21	23	suitable	suitable
25	3	become	became